A modal analysis method to study fluid-structure coupling in hollow parts of a structure

Sébastien Besset, Louis Jezequel

A MODAL ANALYSIS METHOD TO STUDY FLUID-STRUCTURE COUPLING IN HOLLOW PARTS OF A STRUCTURE

S. BESSET and L. JÉZÉQUEL
D2S, LTDS, École Centrale de Lyon
36, avenue Guy de Collongue, 69134 Ecully cedex, France

Journal of Computational Acoustics, 16(2), 257-277, 2008

Abstract

Complex structures often include hollow parts. These hollow parts constitute the skeleton of the structure and are largely responsible for its global behavior, hence the importance of analyzing them precisely. The method we propose in this paper is a modal method based on the modal analysis of elements of hollow parts. This method does not require nodal degrees of freedom on the boundaries between the elements: "modal" elements are created, and these elements can be assembled through modal mass and stiffness matrices in the same way as the finite element method. Thus, it is possible to choose the precision of the analysis by choosing the quantity of modes used in the modal analysis of the elements. We will study not only structural systems but also coupled fluid-structure systems, and our results will be compared with experimental tests.

keywords: Modal analysis; Substructuring; Fluid-structure coupling.

1 Introduction

Complex structures often include hollow parts. The behavior of these hollow parts is quite important for it is greatly responsible for the behavior of the whole structure. Indeed, hollow parts constitute the skeleton of many complex structures, such as cars. Moreover, they are also usually associated with plates. In this case, they are considered as stiffeners. These stiffeners can be studied using a finite element model based on the real geometry of the structure. This is a quite expensive method because it requires many degrees of freedom to be sufficiently precise. Hollow parts can also be considered as beams. Several beam models do exist, but they are not always capable of representing the real characteristics of the geometry.

A modal substructuring method has already been proposed to describe hollow parts [1]. This method uses modes corresponding to each side of a stiffener element of length δz. The hollow parts of the structure can be described by these modes. Assembly of

the stiffener elements is done through the generalized degrees of freedom. Thus, no nodal degrees of freedom are required on the boundaries. However, nodal degrees of freedom have to be kept in order to assemble the hollow part to the rest of the structure.

Acoustical coupling inside hollow parts is also very important. Hollow parts can be considered as wave guides and propagate noise. In order to predict the acoustical behavior of a structure, it is necessary to take coupling into account. Modal analysis of coupled fluid-structure systems has already been studied [2, 3, 4]. The method we propose here will use acoustical and structural modes to describe the hollow parts.

The hollow part will be divided into several elements. Each element will be analyzed as a coupled fluid-structure system. Particular modes will be chosen in order to allow assembly of these elements without the use of nodal degrees of freedom.

We will first explain the method examining a hollow part *in vacuo*. Through several examples, we will compare our results with finite element methods. The case of an infinite waveguide will be reviewed. A hollow part will then be coupled to a plate, in order to show how different structures can be assembled. In this case, the hollow part is considered as a stiffener. To assemble a hollow part with another structure, we will use the "Double Modal Synthesis" method proposed by Jezequel [5, 6, 7]. Thus, the stiffeners coupled to the plate will be represented by "branch modes", which are generalized degrees of freedom corresponding to the boundaries between the structures.

We will then study the case of an acoustical coupling inside the hollow part. Results will be compared with a finite element model and a test. This last example will show that the method proposed in this paper is able to take into account acoustics problems. Indeed, hollow parts constituting the skeleton of a complex structure can be responsible for noise propagation, because these hollow parts can be considered as wave guides. It is important to be able to predict this noise. To do this, the acoustical aspects of the hollow parts must be quite precisely represented.

2 Analysis of hollow parts of a structure *in vacuo*

The hollow part we wish to study is shown on figure 1. This structure will be divided into several elements. Each element is meshed with boundary degrees of freedom only, as shown in figure 2. It is not actually necessary to remove the internal degrees of freedom, but it will facilitate the explanation of the method. Note that internal degrees of freedom should be expressed as a function of internal modes, using the Craig & Bampton method for example [8].

2.1 Modal analysis of an element

Figure 2 shows an element used to analyze the hollow part. When the modal analysis of this element is complete, two nodal degrees of freedom will remain, in order to couple the hollow part with another structure. The behavior of an element can be described with the equation of motion:

$$\left(-\omega^2 \begin{bmatrix} \mathbf{M}_{LL} & \mathbf{M}_{LR} \\ \mathbf{M}_{RL} & \mathbf{M}_{RR} \end{bmatrix} + \begin{bmatrix} \mathbf{K}_{LL} & \mathbf{K}_{LR} \\ \mathbf{K}_{RL} & \mathbf{K}_{RR} \end{bmatrix}\right) \begin{Bmatrix} \mathbf{u}_L \\ \mathbf{u}_R \end{Bmatrix} = \begin{Bmatrix} \mathbf{f}_L \\ \mathbf{f}_R \end{Bmatrix} \quad (1)$$

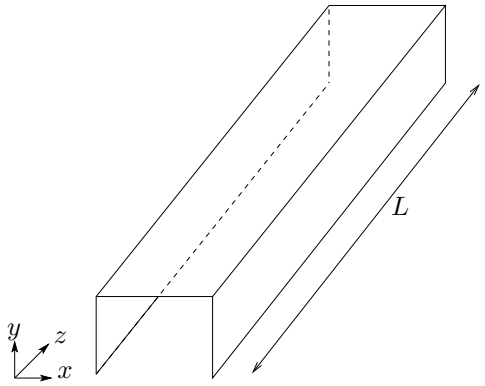

Figure 1: Hollow part to study

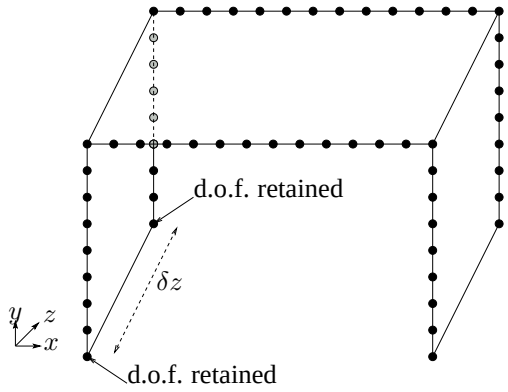

Figure 2: Element of the hollow part

where mass and stiffness matrices $\mathbf{M}$ and $\mathbf{K}$ are split into left and right degrees of freedom L and R. Vectors $\mathbf{u}$ and $\mathbf{f}$ are split the same way.

$\mathbf{u}_L$ and $\mathbf{u}_R$ are then split into degrees of freedom that will be expressed as a function of generalized degrees of freedom $\mathbf{u}_L^g$ and $\mathbf{u}_R^g$, and the others $\mathbf{u}_L^k$ and $\mathbf{u}_R^k$ – marked "retained" on figure 2:

$$\mathbf{u}_L = \left\{ \begin{array}{c} \mathbf{u}_L^k \\ \mathbf{u}_L^g \end{array} \right\}, \qquad \mathbf{u}_R = \left\{ \begin{array}{c} \mathbf{u}_R^k \\ \mathbf{u}_R^g \end{array} \right\} \tag{2}$$

Let ϕ_R be the matrix of the modes of the element when one node of the right side is fixed, as shown in figure 3.

Φ_R is the modal matrix corresponding to right nodes of the element – it is a part of matrix ϕ_R. According to the Craig & Bampton theory [8], displacements of these right nodes can be expressed as follows:

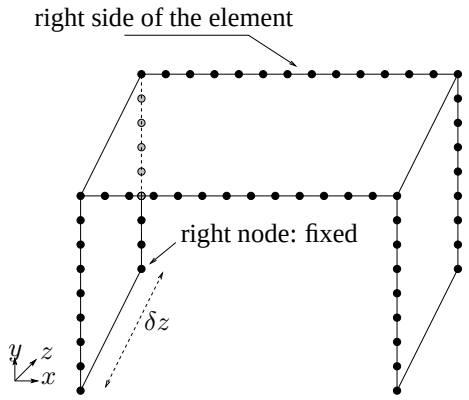

Figure 3: Element of a hollow part

$$\mathbf{u}_R^g = \Phi_R \mathbf{q}_R + \Psi_R \mathbf{u}_R^k \tag{3}$$

where Ψ_R is the matrix of the static modes, corresponding to the rigid body modes of the right side of the element.

Analogous matrices are defined for the left side of the element. Let ϕ_L be the matrix of the modes of the element when one node of the left side is fixed. Φ_L is the modal matrix corresponding to left nodes of the element. Displacements of these left nodes can be expressed as follows:

$$\mathbf{u}_L^g = \Phi_L \mathbf{q}_L + \Psi_L \mathbf{u}_L^k \tag{4}$$

Thus, displacements $\mathbf{u}$ can be expressed as a function of generalized degrees of freedom $\mathbf{q}_L$ and $\mathbf{q}_R$:

$$\begin{Bmatrix} \mathbf{u}_L^k \\ \mathbf{u}_L^g \\ \mathbf{u}_R^k \\ \mathbf{u}_R^g \end{Bmatrix} = \begin{bmatrix} \mathbf{I} & \mathbf{0} & \mathbf{0} & \mathbf{0} \\ \Psi_L & \Phi_L & \mathbf{0} & \mathbf{0} \\ \mathbf{0} & \mathbf{0} & \mathbf{I} & \mathbf{0} \\ \mathbf{0} & \mathbf{0} & \Psi_R & \Phi_R \end{bmatrix} \begin{Bmatrix} \mathbf{u}_L^k \\ \mathbf{q}_L \\ \mathbf{u}_R^k \\ \mathbf{q}_R \end{Bmatrix} \tag{5}$$

Notice that as left degrees of freedom do not depend on right modes, and right degrees of freedom do not depend on left modes, assembling modal elements will be possible.

2.2 Assembling elements

In order to assemble two elements, let write the relations between the nodal degrees of freedom of the left and right side of two elements. Degrees of freedom of the right side of the first element, called $\mathbf{u}_{R1}^k$ and $\mathbf{u}_{R1}^g$, must match with degrees of freedom of the left side of the second element, called $\mathbf{u}_{L2}^k$ and $\mathbf{u}_{L2}^g$:

$$\left\{ \begin{array}{l} \mathbf{u}_{R1}^{k} = \mathbf{u}_{L2}^{k} \\ \mathbf{u}_{R1}^{g} = \mathbf{u}_{L2}^{g} \end{array} \right. \tag{6}$$

Equation 6 can be written for elements n and $n+1$:

$$\left\{ \begin{array}{l} \mathbf{u}_{R_n}^{k} = \mathbf{u}_{L_{n+1}}^{k} \\ \mathbf{u}_{R_n}^{g} = \mathbf{u}_{L_{n+1}}^{g} \end{array} \right. \tag{7}$$

Equations 6 leads to the expression of degrees of freedom of the left part of the second element as a function of degrees of freedom of the first element:

$$\left\{ \begin{array}{l} \mathbf{u}_{L2}^{k} = \mathbf{u}_{R1}^{k} \\ \mathbf{q}_{L2} = \tilde{\Phi}_L \left(\Phi_R \mathbf{q}_{R1} + \left(\Psi_R - \Psi_L \right) \mathbf{u}_{R1}^{k} \right) \end{array} \right. \tag{8}$$

which can be written for elements n and $n+1$:

$$\left\{ \begin{array}{l} \mathbf{u}_{L_{n+1}}^{k} = \mathbf{u}_{R_n}^{k} \\ \mathbf{q}_{L_{n+1}} = \tilde{\Phi}_L \left(\Phi_R \mathbf{q}_{R_n} + \left(\Psi_R - \Psi_L \right) \mathbf{u}_{R_n}^{k} \right) \end{array} \right. \tag{9}$$

where $\tilde{\Phi}_L$ is a pseudo-inverse matrix of Φ_L:

$$\tilde{\Phi}_L = \left(\Phi_L^T \Phi_L \right)^{-1} \Phi_L^T \tag{10}$$

Equations 8 allow the assembling of N elements, using transfer matrices $\mathbf{T}_n$:

$$\mathbf{K}_{\text{tot}} = \sum_{n=1}^{N} \mathbf{T}_n^T \mathbf{K} \mathbf{T}_n \tag{11}$$

$$\mathbf{M}_{\text{tot}} = \sum_{n=1}^{N} \mathbf{T}_n^T \mathbf{M} \mathbf{T}_n \tag{12}$$

Notice that assembling matrices is as simple as in the finite element method. For two elements, matrices $\mathbf{T}_n$ are built as follows:

$$\mathbf{T}_1 = \begin{bmatrix} \mathbf{I} & \mathbf{0} & \mathbf{0} & \mathbf{0} & \mathbf{0} & \mathbf{0} \\ \mathbf{0} & \mathbf{I} & \mathbf{0} & \mathbf{0} & \mathbf{0} & \mathbf{0} \\ \mathbf{0} & \mathbf{0} & \mathbf{I} & \mathbf{0} & \mathbf{0} & \mathbf{0} \\ \mathbf{0} & \mathbf{0} & \mathbf{0} & \mathbf{I} & \mathbf{0} & \mathbf{0} \end{bmatrix} \tag{13}$$

$$\mathbf{T}_2 = \begin{bmatrix} \mathbf{0} & \mathbf{0} & \mathbf{I} & \mathbf{0} & \mathbf{0} & \mathbf{0} \\ \mathbf{0} & \mathbf{0} & \tilde{\Phi}_L \left(\Psi_R - \Psi_L \right) & \tilde{\Phi}_L \Phi_R & \mathbf{0} & \mathbf{0} \\ \mathbf{0} & \mathbf{0} & \mathbf{0} & \mathbf{0} & \mathbf{I} & \mathbf{0} \\ \mathbf{0} & \mathbf{0} & \mathbf{0} & \mathbf{0} & \mathbf{0} & \mathbf{I} \end{bmatrix} \tag{14}$$

Notice that it is possible to use equation 14 for matrix $\mathbf{T}_1$. Matrix given in equation 11 is more simple, but it may be easier to use the same kind of matrix for each element. Thus, for N elements, matrices $\mathbf{T}_n$ can be written:

$$\mathbf{T}_n = \begin{bmatrix} \mathbf{0} & \cdots & \mathbf{0} & \mathbf{I} & \mathbf{0} & \mathbf{0} & \mathbf{0} & \mathbf{0} & \cdots & \mathbf{0} \\ \mathbf{0} & \cdots & \mathbf{0} & \tilde{\Phi}_L(\Psi_R - \Psi_L) & \tilde{\Phi}_L\Phi_R & \mathbf{0} & \mathbf{0} & \mathbf{0} & \cdots & \mathbf{0} \\ \mathbf{0} & \cdots & \mathbf{0} & \mathbf{0} & \mathbf{0} & \mathbf{I} & \mathbf{0} & \mathbf{0} & \cdots & \mathbf{0} \\ \mathbf{0} & \cdots & \mathbf{0} & \mathbf{0} & \mathbf{0} & \mathbf{0} & \mathbf{I} & \mathbf{0} & \cdots & \mathbf{0} \end{bmatrix} \tag{15}$$

$$\underbrace{\qquad\qquad}_{2(n-1)\text{ columns}} \qquad\qquad \underbrace{\qquad\qquad}_{2(N-n)\text{ columns}} \tag{16}$$

Equation 15 is valid for $n = 1 \ldots N$. For $n = 1$, it is also possible to use matrix $\mathbf{T}_1$ defined as follows:

$$\mathbf{T}_1 = \begin{bmatrix} \mathbf{I} & \mathbf{0} & \mathbf{0} & \mathbf{0} & \mathbf{0} & \cdots & \mathbf{0} \\ \mathbf{0} & \mathbf{I} & \mathbf{0} & \mathbf{0} & \mathbf{0} & \cdots & \mathbf{0} \\ \mathbf{0} & \mathbf{0} & \mathbf{I} & \mathbf{0} & \mathbf{0} & \cdots & \mathbf{0} \\ \mathbf{0} & \mathbf{0} & \mathbf{0} & \mathbf{I} & \mathbf{0} & \cdots & \mathbf{0} \end{bmatrix} \tag{17}$$

$$\underbrace{\qquad\qquad}_{2(N-1)\text{ columns}} \tag{18}$$

Notice that if the hollow part is a periodic structure, there is a relation between matrices Φ_L and Φ_R:

$$\Phi_R = \mathbf{A}\Phi_L \tag{19}$$

where $\mathbf{A}$ is a diagonal matrix defined as follows:

$$\begin{aligned} &\mathbf{A}(i,i) = -1 \quad \text{if } i \text{ is associated with :} && -\text{ the } z \text{ translation} \\ &&& -\text{ the } x \text{ rotation} \\ &&& -\text{ the } y \text{ rotation} \\ &\mathbf{A}(i,i) = 1 \qquad \text{else} \end{aligned} \tag{20}$$

Matrices Ψ_L and Ψ_R correspond to rigid body modes of the element, since only one node is fixed. Hence the relation:

$$\Psi_L = \Psi_R \tag{21}$$

Equations 19 and 21 allow the transfer matrices $\mathbf{T}_n$ to be simplified.

2.3 Coupling structures using "double modal synthesis"

The "hollow parts" that have been studied in the previous sections are parts of a complex structure including plates and stiffeners. During the modal analysis of the elements constituting these hollow parts, nodal degrees of freedom have been retained. The nodes kept fixed in the modal analysis of the elements allow us to couple the hollow part with another structure – a plate, for example. Thus, the second structure is studied using a classic modal analysis method – the Craig & Bampton method for example. Coupling is made through the nodal degrees of freedom remaining from the modal analysis.

In order to use only generalized degrees of freedom, it is possible to express degrees of freedom of the boundary between the two structures as a function of "branch

modes", using the "double modal synthesis" method [5, 6, 7]. Looking at the coupled problem, the motion equation can be written as follows:

$$\left(-\omega^2 \begin{bmatrix} \mathbf{M}_{HH} & \mathbf{M}_{HB} & \mathbf{M}_{HS} \\ \mathbf{M}_{BH} & \mathbf{M}_{BB} & \mathbf{M}_{BS} \\ \mathbf{M}_{SH} & \mathbf{M}_{SB} & \mathbf{M}_{SS} \end{bmatrix} + \begin{bmatrix} \mathbf{K}_{HH} & \mathbf{K}_{HB} & \mathbf{K}_{HS} \\ \mathbf{K}_{BH} & \mathbf{K}_{BB} & \mathbf{K}_{BS} \\ \mathbf{K}_{SH} & \mathbf{K}_{SB} & \mathbf{K}_{SS} \end{bmatrix} \right) \begin{Bmatrix} \mathbf{q}_H \\ \mathbf{u}_B \\ \mathbf{q}_S \end{Bmatrix} = \mathbf{f} \tag{22}$$

We denote H the generalized degrees of freedom concerning the hollow part, B the nodal degrees of the boundary, and S the generalized degrees of freedom of the second structure. $\mathbf{f}$ is the vector of the generalized forces applied on the system.

Φ_B is the matrix of the branch modes, which satisfy the following equation:

$$\left(-\left[\omega_i^2\right] \mathbf{M}_{BB} + \mathbf{K}_{BB} \right) \Phi_B = \mathbf{0} \tag{23}$$

where $\left[\omega_i^2\right]$ $(1 < i < N)$ is a diagonal matrix of N eigenfrequencies. Boundary degrees of freedom $\mathbf{u}_B$ can be expressed as follows:

$$\mathbf{u}_B = \Phi_B \mathbf{q}_B \tag{24}$$

which allow the whole system to be fully described with generalized degrees of freedom: "Section modes" for the hollow parts, "surface modes for the plates", and "branch modes" for the boundaries between the hollow parts and the plates.

2.4 Results *in vacuo*

2.4.1 Analysis of an infinite waveguide

The first comparison was made for an infinite waveguide. We consider the hollow part as an infinite and periodic structure. Mass and stiffness matrices are divided into left and right sides. We compute the dispersion curves for this infinite waveguide using finite element matrices (denoted $\mathbf{M}$ and $\mathbf{K}$) and modal matrices (computed using our proposed method and denoted $\overline{\mathbf{M}}$ and $\overline{\mathbf{K}}$).

Considering equation 27, which is the motion equation of an element (properties in table 1 and 2), we use the following notation:

$$\mathbf{Z}(\omega) = -\omega^2 \mathbf{M} + \mathbf{K} \tag{25}$$

$$\overline{\mathbf{Z}}(\omega) = -\omega^2 \overline{\mathbf{M}} + \overline{\mathbf{K}} \tag{26}$$

$$\begin{bmatrix} \mathbf{Z}_{LL}(\omega) & \mathbf{Z}_{LR}(\omega) \\ \mathbf{Z}_{RL}(\omega) & \mathbf{Z}_{RR}(\omega) \end{bmatrix} \begin{Bmatrix} \mathbf{u}_L \\ \mathbf{u}_R \end{Bmatrix} = \begin{Bmatrix} \mathbf{f}_L \\ \mathbf{f}_R \end{Bmatrix} \tag{27}$$

The modal equation corresponding to equation 27 can be written:

$$\begin{bmatrix} \overline{\mathbf{Z}}_{LL}(\omega) & \overline{\mathbf{Z}}_{LR}(\omega) \\ \overline{\mathbf{Z}}_{RL}(\omega) & \overline{\mathbf{Z}}_{RR}(\omega) \end{bmatrix} \begin{Bmatrix} \mathbf{q}_L \\ \mathbf{q}_R \end{Bmatrix} = \begin{Bmatrix} \overline{\mathbf{f}}_L \\ \overline{\mathbf{f}}_R \end{Bmatrix} \tag{28}$$

Young's modulus	Poisson's ratio	Density
$2.0e11$ Pa	0.33	7850 kg.m^{-3}

Table 1: Properties of the material

Thickness	Section	Length
0.01 m	1×1 m^2	infinite

Table 2: Geometry of the structure

The structure is periodic, hence the relation:

$$\mathbf{u}_R = \alpha \mathbf{u}_L \tag{29}$$
$$\mathbf{f}_R = -\alpha \mathbf{f}_L \tag{30}$$

where $\alpha = e^{-ik\Delta l}$. Real and imaginary parts of $k = k_R + ik_I$ can be written as a function of α as follows:

$$\begin{cases} k_R = \Re(k) = -\dfrac{\arg(\alpha)}{\Delta l} \\ k_I = \Im(k) = \dfrac{\ln(|\alpha|)}{\Delta l} \end{cases} \tag{31}$$

Equation 27 becomes:

$$\begin{bmatrix} \mathbf{Z}_{LL}(\omega) & -\mathbf{I} \\ \mathbf{Z}_{RL}(\omega) & \mathbf{0} \end{bmatrix} \begin{Bmatrix} \mathbf{u}_L \\ \mathbf{f}_L \end{Bmatrix} = \alpha \begin{bmatrix} -\mathbf{Z}_{LR}(\omega) & \mathbf{0} \\ -\mathbf{Z}_{RR}(\omega) & -\mathbf{I} \end{bmatrix} \begin{Bmatrix} \mathbf{u}_L \\ \mathbf{f}_L \end{Bmatrix} \tag{32}$$

Considering modal matrices, the equation can be written:

$$\begin{bmatrix} \overline{\mathbf{Z}}_{LL}(\omega) & -\mathbf{I} \\ \overline{\mathbf{Z}}_{RL}(\omega) & \mathbf{0} \end{bmatrix} \begin{Bmatrix} \mathbf{q}_L \\ \overline{\mathbf{f}}_L \end{Bmatrix} = \alpha \begin{bmatrix} -\overline{\mathbf{Z}}_{LR}(\omega)\mathbf{B} & \mathbf{0} \\ -\overline{\mathbf{Z}}_{RR}(\omega)\mathbf{B} & -\mathbf{C} \end{bmatrix} \begin{Bmatrix} \mathbf{q}_L \\ \overline{\mathbf{f}}_L \end{Bmatrix} \tag{33}$$

where $\mathbf{B}$ and $\mathbf{C}$ are matrices coming from the modal synthesis of an element. These matrices allow us to write the equations between $\mathbf{q}_R$ and $\mathbf{q}_L$, and $\overline{\mathbf{f}}_R$ and $\overline{\mathbf{f}}_L$:

$$\mathbf{q}_R = \alpha \mathbf{B} \mathbf{q}_L \tag{34}$$
$$\overline{\mathbf{f}}_R = -\alpha \mathbf{C} \overline{\mathbf{f}}_L \tag{35}$$

$\overline{\mathbf{f}}_R$ and $\overline{\mathbf{f}}_L$ are the modal forces associated with the modal matrices $\overline{\mathbf{M}}$ and $\overline{\mathbf{K}}$.

Propagation curves give k as a function of $f = \dfrac{\omega}{2\pi}$ (k must be real).

The curves obtained from the finite element matrices are given in figure 4. The curves obtained from the modal matrices are given in figures 5, 6 and 7.

Figure 5 is a plot using a modal element of 10 modes. The results are quite poor, which is why we plot the same curves using 30 and 60 modes. Figure 6 shows the

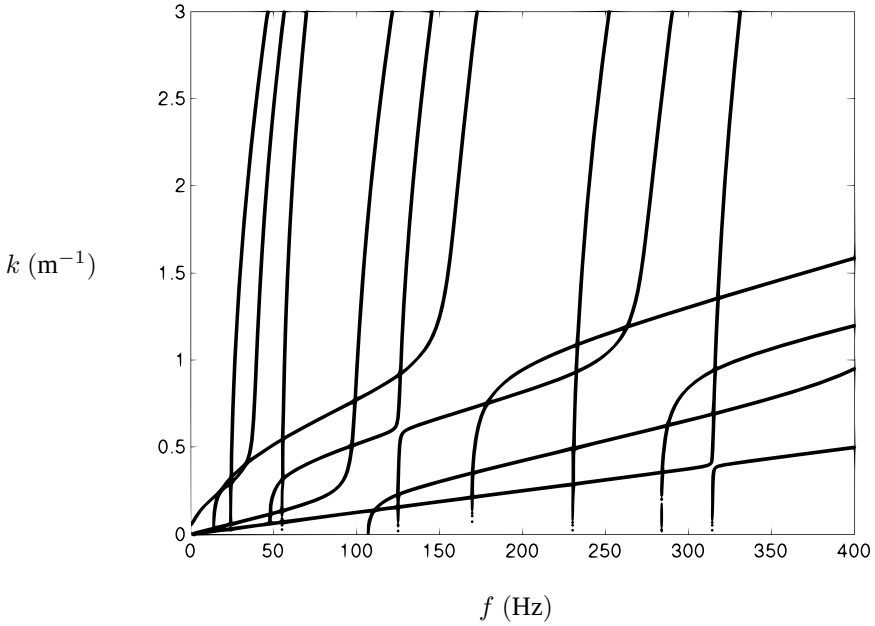

Figure 4: Propagation curves – FEM model

results obtained using 30 modes for an element. Dispersion curves are somewhat better. Figure 7 gives the results obtained using 60 modes for an element. The results are good – at low frequencies, curves are even exactly the same –, but many modes were required.

The need for many generalized degrees of freedom to represent an infinite wave guide can be explained by the fact that the boundaries between elements is the only parameter used in the calculations. In the case of a finite hollow part, stationary waves are generated thanks to the boundary conditions at the beginning and the end of the hollow part. Results should then be better for such cases.

2.4.2 Modal and finite element analysis of a tube

We consider the tube shown in figure 1 split into elements shown in figure 2. This tube may be a hollow part of a structure.

The material used for this comparison is structural steel, whose properties are given in table 3. Properties of the studied structure are given in table 4. The structure is represented in figure 8.

Table 5 shows the eigenfrequencies found by the modal analysis using the method we propose and a finite element method. The finite element model uses 144 degrees of freedom for each section, whereas the modal model uses only 41 degrees of freedom (35 section modes and 6 nodal d.o.f. for each section). The results are quite good.

Figure 9 shows the evolution of the accuracy of the method as a function of the

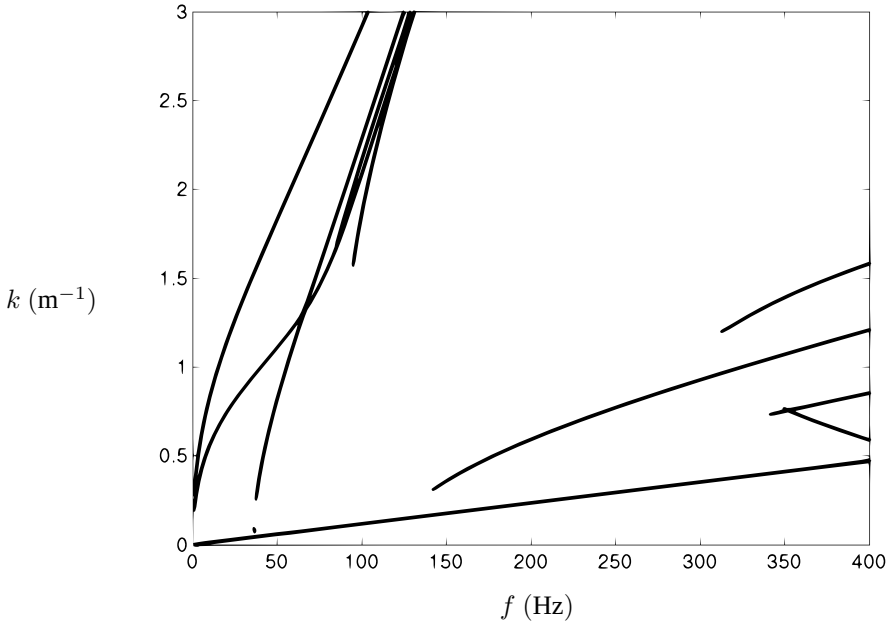

Figure 5: Propagation curves – 10 modes

Young's modulus	Poisson's ratio	Density
$2.0e11$ Pa	0.33	7850 kg.m^{-3}

Table 3: Properties of the material

Thickness	Section	Length
0.001 m	0.1×0.1 m^2	0.2 m

Table 4: Geometry of the structure

number of section modes retained. In this figure, one can see that the results are much more accurate when the number of section modes retained is high. However, the number of section modes need not be as high as in the example given in section 2.4.1. Indeed, the stationary waves make the results more accurate thanks to the boundary conditions.

2.4.3 Stiffener coupled with a plate

We also made calculations using a stiffener coupled with a plate. The whole structure is given in figure 10. The properties of the material and the geometry of the structure are given in tables 6 and 7.

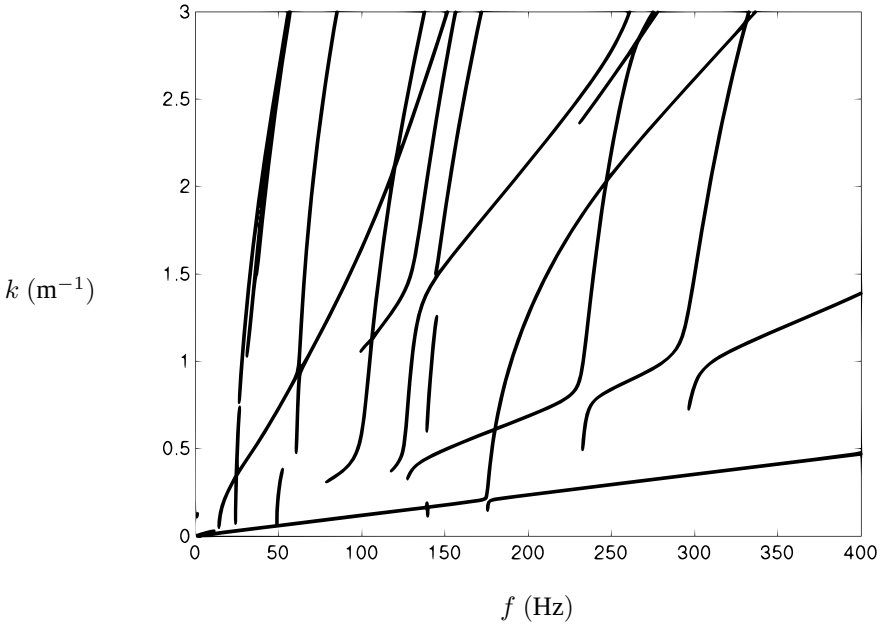

Figure 6: Propagation curves – 30 modes

Frequencies found by a classical finite element method – 144 × 25 d.o.f. – (Hz)	Frequencies found by proposed method – 41 × 25 d.o.f. – (Hz) (35 modes for each section)	Error (%)
138.0	137.9	0.08
141.4	141.9	0.36
240.4	239.0	0.62
249.8	247.3	0.99
282.5	272.6	3.6
312.0	315.5	1.1
321.9	375.8	14.3
335.7	392.0	14.3
401.8	393.6	2.1
408.3	424.4	3.8
411.6	425.2	3.2
444.4	455.2	2.3

Table 5: Eigenfrequencies of the hollow part

This case is very interesting to study because hollow parts are often used as stiffeners. Coupled to a plate, such stiffeners are useful to modify the characteristics of the structure and the values of its eigenfrequencies.

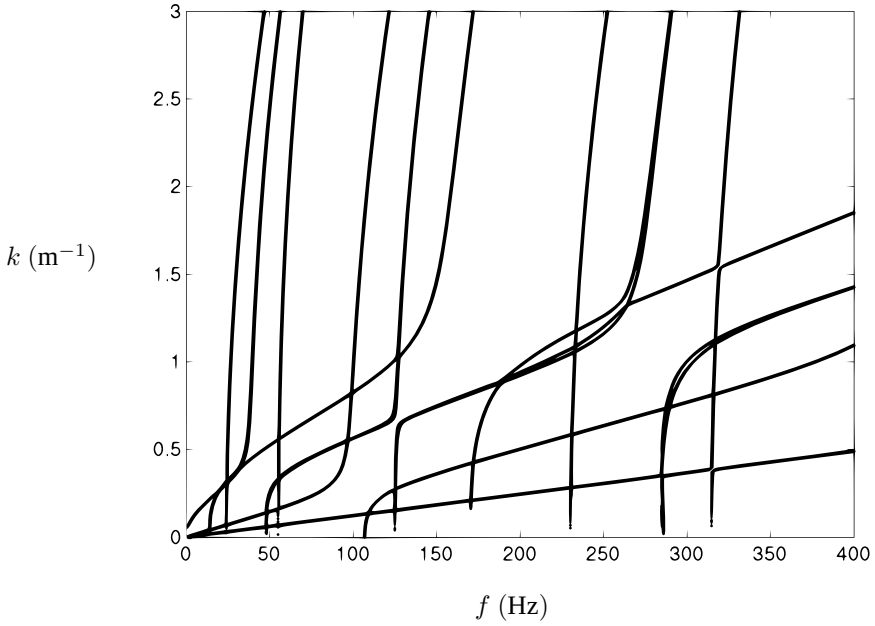

Figure 7: Propagation curves – 60 modes

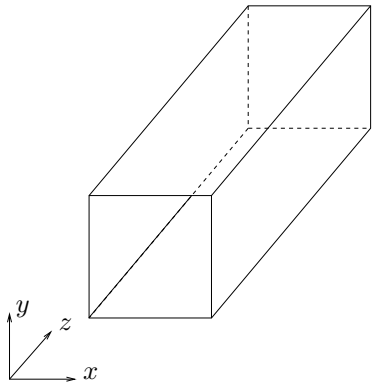

Figure 8: Studied structure

Young's modulus	Poisson's ratio	Density
$2.0e11$ Pa	0.33	7850 kg.m^{-3}

Table 6: Properties of the material

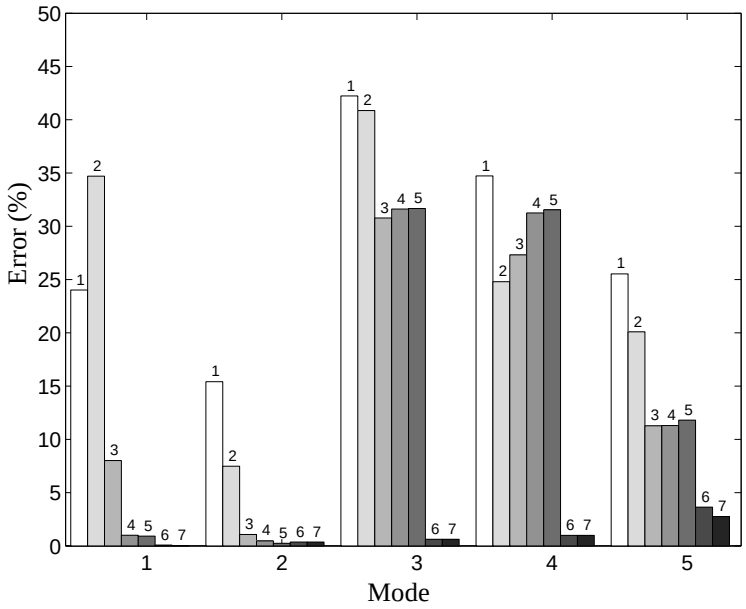

Figure 9: Error on the first modes as a function of the number of section modes retained (1: 10 modes, 2: 15 modes, 3: 20 modes, 4: 25 modes, 5: 30 modes, 6: 35 modes, 7: 40 modes)

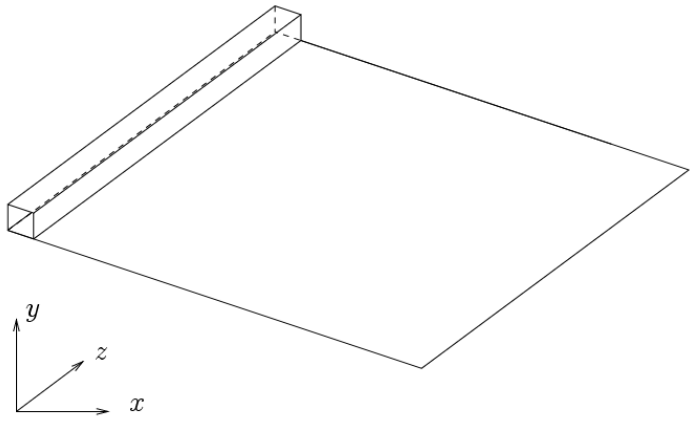

Figure 10: Hollow part coupled with a plate

We compute the eigenfrequencies of the whole structure. These eigenfrequencies have been calculated using three methods: a finite element method (considered as a

Thickness	Section	Hollow part length	Plate
0.001 m	0.1×0.1 m^2	0.5 m	1.2×0.5 m^2

Table 7: Geometry of the structure

reference), the modal method we propose, and a method using beam modeling. The results show that the method we propose is quite close to the finite element method. Figures 11 and 12 shows the error between our method and the finite element method, and between the method using Timoshenko beam modeling and the finite element method. In this example, we first used 10 generalized degrees of freedom (figure 11), and then 50 generalized degrees of freedom (figure 12) for each element of the stiffener. Using 50 modes provides better results, but the difference between 10 and 50 section modes is quite small. In both cases, the modal method we propose gives better results than a method using Timoshenko beam modeling. Notice that for the case of coupled structures, the number of section modes retained is not as important as for the single beam studied in section 2.4.2. Indeed, the behavior of the structure does not depend only on the stiffener, but also on the plate, which is why the accuracy of the analysis of the stiffener is not as important as for the first example (given in section 2.4.2).

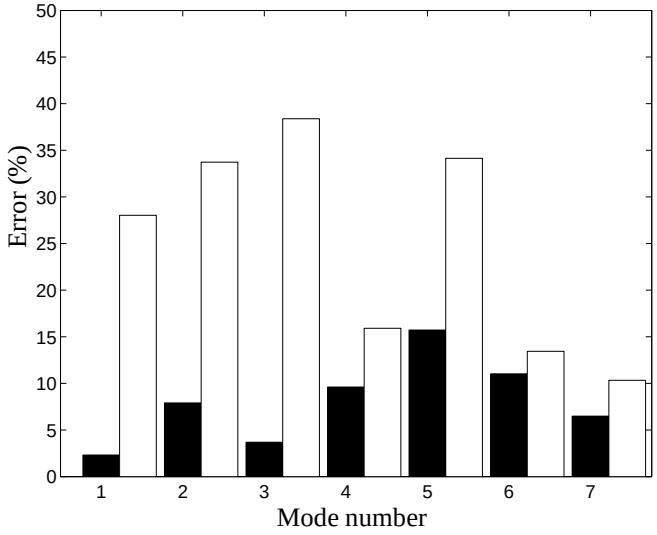

Figure 11: Error compared to finite element method (black: using 10 section modes for each element of the stiffener, white: using beam modeling)

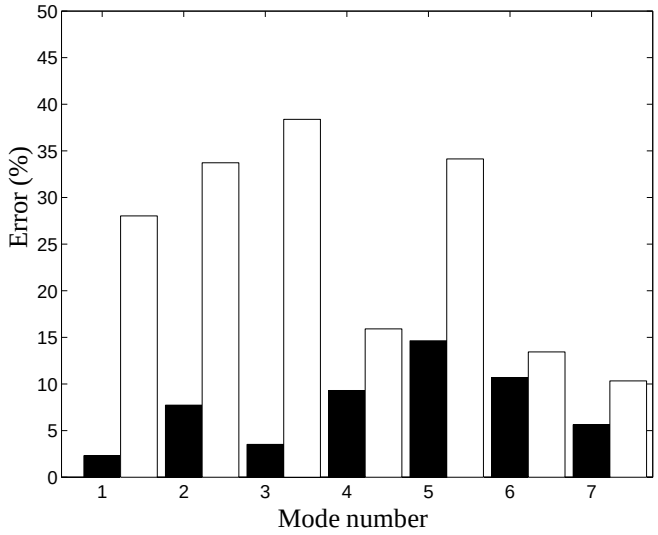

Figure 12: Error compared to finite element method (black: using 50 section modes for each element of the stiffener, white: using a beam modeling)

3 Analysis of a hollow part including fluid-structure coupling

In this section, the hollow part considered in section 2 will be studied considering the acoustical aspects.

3.1 Modal analysis of an element

The hollow parts of the structure are split into several elements, as for the *in vacuo* case.

Fluid-structure problems have often been studied and equations concerning acoustical coupling are well known [3, 4, 9]. Using a finite element formulation, the motion equation of an element can be written as follows:

$$\left(-\omega^2 \begin{bmatrix} \mathbf{M}_S & \mathbf{0} \\ \mathbf{C} & \mathbf{M}_A \end{bmatrix} + \begin{bmatrix} \mathbf{K}_S & -\mathbf{C}^T \\ \mathbf{0} & \mathbf{K}_A \end{bmatrix}\right) \begin{Bmatrix} \mathbf{u} \\ \mathbf{p} \end{Bmatrix} = \begin{Bmatrix} \mathbf{f} \\ \mathbf{0} \end{Bmatrix} \tag{36}$$

The method we use to study the coupled system is the same as for the *in vacuo* problem. Modes of the fluid part will first be calculated and then an analysis of the structural part will be performed.

3.1.1 Analysis of the fluid part

In order to find modes allowing us to easily assemble elements, let us split the acoustical mass and stiffness matrices into left and right sides of an element:

$$\mathbf{M}_A = \begin{bmatrix} \mathbf{M}_{ALL} & \mathbf{M}_{ALR} \\ \mathbf{M}_{ARL} & \mathbf{M}_{ARR} \end{bmatrix} \tag{37}$$

$$\mathbf{K}_A = \begin{bmatrix} \mathbf{K}_{ALL} & \mathbf{K}_{ALR} \\ \mathbf{K}_{ARL} & \mathbf{K}_{ARR} \end{bmatrix} \tag{38}$$

The pressure vector $\mathbf{p}$ is split the same way:

$$\mathbf{p} = \begin{Bmatrix} \mathbf{p}_L \\ \mathbf{p}_R \end{Bmatrix} \tag{39}$$

First, the modal matrix ϕ_R^A is introduced. It is the matrix of the acoustical modes of an element when one node of the right side is fixed ($\mathbf{p}_R^k = 0$) (see figure 3 for notations). Φ_R^A is the part of matrix ϕ_R^A concerning the nodes of the right side of the element.

Secondly, matrix Φ_L^A is the matrix of the acoustical modes of an element when one node of the left side is fixed ($\mathbf{p}_L^k = 0$). Φ_L^A is the part of matrix Φ_L^A concerning the nodes of the left side of the element.

Pressure vector $\mathbf{p}$ can be written as a function of generalized degrees of freedom $\mathbf{q}_L^A$ and $\mathbf{q}_R^A$ and pressure on fixed nodes $\mathbf{p}_R^k$ and $\mathbf{p}_L^k$:

$$\mathbf{p}_L^g = \Phi_L^A \mathbf{q}_L^A + \Psi_L^A \mathbf{p}_L^k \tag{40}$$

$$\mathbf{p}_R^g = \Phi_R^A \mathbf{q}_R^A + \Psi_R^A \mathbf{p}_R^k \tag{41}$$

Notice that generalized degrees of freedom of each side of the element only depend on nodal degrees of freedom of the same side, which will allow us to easily assemble elements.

3.1.2 Analysis of the structural part

The modal analysis of the structural part of a element has already been given in section 2.1. Using similar notations, displacements of the two sides of an element can be expressed as follow:

$$\mathbf{u}_L^g = \Phi_L \mathbf{q}_L + \Psi_L \mathbf{u}_L^k \tag{42}$$

$$\mathbf{u}_R^g = \Phi_R \mathbf{q}_R + \Psi_R \mathbf{u}_R^k \tag{43}$$

As for the acoustical analysis, generalized degrees of freedom of each side of the element depend only on nodal degrees of freedom of the same side.

3.2 Assembling elements

In order to assemble two elements, let us write the relations between the right side of the n^{th} element and the left side of the $(n+1)^{\text{th}}$ element:

$$\begin{cases} \mathbf{u}^k_{L_{n+1}} = \mathbf{u}^k_{R_n} \\ \mathbf{u}^g_{L_{n+1}} = \mathbf{u}^g_{R_n} \\ \mathbf{p}^k_{L_{n+1}} = \mathbf{p}^k_{R_n} \\ \mathbf{p}^g_{L_{n+1}} = \mathbf{p}^g_{R_n} \end{cases} \tag{44}$$

Using equations 40, 41, 42 and 43, equation 44 leads to:

$$\begin{cases} \mathbf{u}^k_{L_{n+1}} = \mathbf{u}^k_{R_n} \\ \mathbf{q}_{L_{n+1}} = \tilde{\Phi}_L \left(\Phi_R \mathbf{q}_{R_n} + \left(\Psi_R - \Psi_L \right) \mathbf{u}^k_{R_n} \right) \\ \mathbf{p}^k_{L_{n+1}} = \mathbf{p}^k_{R_n} \\ \mathbf{q}^A_{L_{n+1}} = \tilde{\Phi}^A_L \left(\Phi^A_R \mathbf{q}_{R_n} + \left(\Psi^A_R - \Psi^A_L \right) \mathbf{p}^k_{R_n} \right) \end{cases} \tag{45}$$

These relations lead to transfer matrices that allow us to assemble several elements, as explain in section 2.2 (equations 11 and 12).

3.3 Results

In this section, we compare the results obtained with our proposed method and experimental tests conducted on a hollow part.

3.3.1 Verification of proposed method

The verification of the modal synthesis method we propose is made using elements shown on figure 17. Our modal synthesis method is now compared with a finite element model. Figure 13 shows the error between these two methods for one elements. This error is quite small and shows the efficiency of the model we propose.

3.3.2 Validation by experimental testing

The hollow part used for the tests is shown in picture 14.

We used a shock hammer for the excitation and a microphone to get the pressure inside the hollow part, as shown in picture 15. Experimental material is shown in picture 16. Of course, the acoustical cavity has been blocked up. It is open in the picture in order to show the microphone.

3.3.3 Modal analysis and comparison

The structure has been studied using the method proposed in the paper. A different element has been used for the curved part. The two kind of elements are shown on figure 17 and 18.

The properties of the material used for this example are given in table 8. The Young's modulus has been matched in order to get the best results possible. The

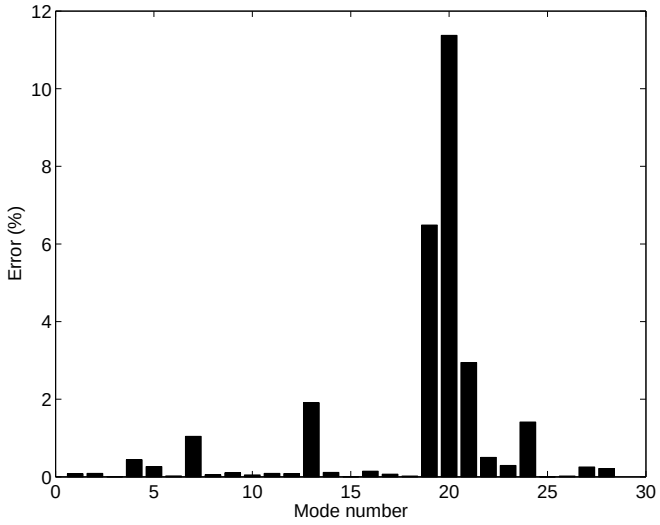

Figure 13: Verification of the method

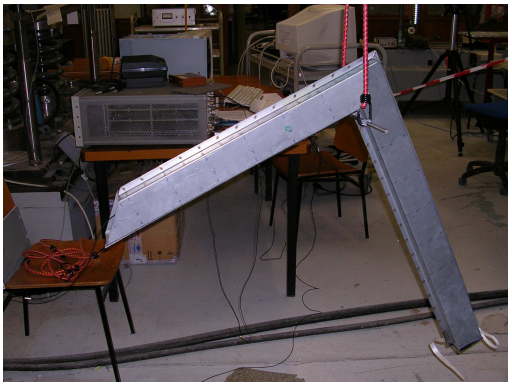

Figure 14: Hollow part used for experimental testing

Young's modulus should be approximately $2.0e11$ Pa. We found an optimal value of $1.96e11$ Pa.

Young's modulus	Poisson's ratio	Density	Section	Length
$1.96e11$ Pa	0.33	7850 kg.m^{-3}	0.08×0.08 m^2	0.9 m / 0.65 m

Table 8: Properties of the material used for testing

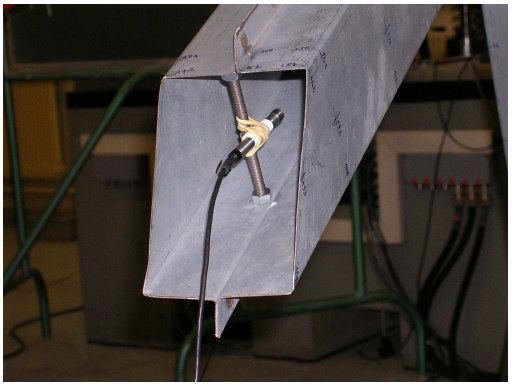

Figure 15: Microphone used for experimental testing

Figure 16: Material used for testing

Figure 19 shows the results obtained in this section. The behavior of the hollow part has been predicted quite well. The measurement curve breaks down at 350 Hz, because of the cut-off frequency of the shock hammer. Nevertheless, the two curves under 350 Hz are not so different.

Under 350 Hz, differences between the two curves may have various reasons. First, the hollow part has been suspended through a rigid bar – in order to get a punctual contact – and a sandow. This sandow induces a very low stiffness that could influence the results. Secondly, though the extremities of the hollow part have been blocked, there may be leakage because of the wire of the microphone. There may also have

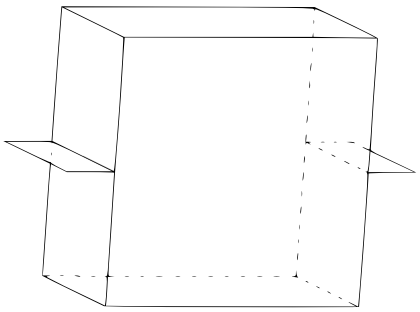

Figure 17: Element used for the modal analysis

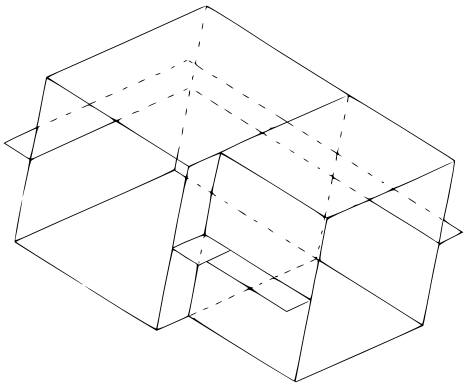

Figure 18: Element used for the modal analysis – curved part

been measurement errors or inaccurate measurements.

4 Conclusion

The method we proposed in this paper allows us to study hollow parts of a structure with good precision, using generalized degrees of freedom. This modal method does not use nodal degrees of freedom on the boundaries between elements, which is quite interesting. Modal matrices created by the modal analysis of an element can be assembled the same way as finite element matrices.

Numerical testing on a waveguide and a finite element model have shown that the method can produce quite good results. Of course, results obtained for the infinite waveguide are not as good as the results obtained with finite hollow parts. The case of a stiffener coupled to a plate has been processed. It has been shown that the method proposed in the paper was able to produce good results in this case. Experimental testing has shown that the fluid-structure coupling was correctly modelized, which will allow

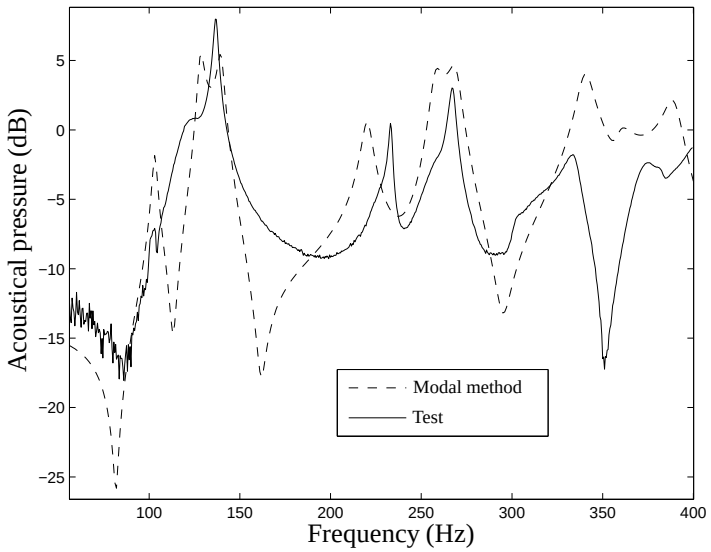

Figure 19: Measurements and modal analysis

us to predict the pressure field resulting from the the skeleton of a complex structure.

Acknowledgement

The authors thank Mr. Stéphane Lemahieu for his help during the experimental works.

References

[1] S. Besset, L. Jezequel, Modal analysis of hollow parts of a structure, in: *IMAC XXIV: A Conference & Exposition on Structural Dynamics*, 2005.

[2] G. E. Sandberg, P.-A. Hansson, M. Gustavsson, Domain decomposition in acoustic and structure-acoustic analysis, *Computer Methods in Applied Mechanics and Engineering* 190 (2001) 2979–2988.

[3] R. Ohayon, Reduced models for fluid-structure interaction problems, *International Journal for Numerical Methods in Engineering* 60 (2003) 139–152.

[4] R. Ohayon, Reduced symmetric models for modal analysis of internal structural-acoustic and hydroelastic-sloshing systems, *Computer Methods in Applied Mechanics and Engineering* 190 (2001) 3009–3019.

[5] L. Jezequel, Procedure to reduce the effects of modal truncation in eigensolution reanalysis, *AIAA journal* 28 (5) (1990) 896–902.

[6] L. Jezequel, Hybrid method of modal synthesis using vibrations tests, *Journal of Sound and Vibration* 100 (2) (1985) 191–210.

[7] L. Jezequel, A method of damping synthesis from substructures tests, *ASME Journal of Mechanical design* 102 (1980) 286–294.

[8] R. R. Craig, M. C. C. Bampton, Coupling of substructures for dynamic analysis, *AIAA Journal* 6 (1968) 1313–1321.

[9] M. C. Junger, Acoustic fluid-elastic structure interactions: Basic concepts, *Computers & Structures* 65 (3) (1997) 287–293.